https://doi.org/10.48048/tis.2025.9249

Roasted-Coffee Aroma Sensing by Using Polymethyl Methacrylate (PMMA) and Polymethyl Methacrylate-Reduced Graphene Oxide (PMMA-rGO) Composite-based Quartz Crystal Microbalance (QCM) Sensor

Ferry Chrismiadi Nalle[1,4], Akhmad Sabarudin[1], Aditya Ilham Saputra[3,4], Alim Romdhoni[3,4], Nike Fitayatul Khusnah[2] and Setyawan Purnomo Sakti[3,4,*]

[1]*Department of Chemistry, Brawijaya University, Malang 65142, Indonesia*
[2]*Integrated Research Laboratory (LRT-UB), Brawijaya University, Malang 65142, Indonesia*
[3]*Department of Physics, Brawijaya University, Malang 65142, Indonesia*
[4]*Sensor Technology Laboratory (SenTLab), Department of Physics, Brawijaya University, Malang 65142, Indonesia*

([*]Corresponding author's e-mail: sakti@ub.ac.id)

Received: 31 October 2024, Revised: 5 December 2024, Accepted: 12 December 2024, Published: 30 January 2025

Abstract

The primary quality of food is often associated with its physical attributes, particularly aroma. Key volatile compounds play a critical role in determining food quality. Coffee as a high-potential commodity in Indonesia and in the world strongly depends on their aroma as a signature for its quality. Several methods have been performed to determine the quality of coffee like cupping methods and chromatography-based technologies. But it depends on the coffee-experts who cannot be replicated by other people because of their subjectivity and still need complex sample processing and lengthy time-analysis. QCM sensor paves the way to solve this problem. By modification of its surface with nanomaterials, QCM sensing performance significantly can be elevated. This study aimed to detect the aroma of roasted coffee using a QCM-based electronic nose sensor. The QCM sensor was coated with aroma-sensitive materials to improve its sensing capabilities, specifically PMMA and PMMA-rGO composites. Both PMMA and PMMA-rGO were synthesized via an *in situ* polymerization method utilizing a binary solvent system in optimized proportions. The surface roughness of the QCM sensor was slightly higher when coated with PMMA-rGO (Sa = 493.68 ± 74.23 nm) compared to PMMA (Sa = 446.02 ± 26.19 nm) alone. The incorporation of rGO significantly enhanced the sensitivity of the QCM sensor towards the roasted coffee aroma. Based on the Sauerbrey calculation, the value of Δf for PMMA is –66.05 ± 28.77 Hz while for PMMA-rGO is –74.28 ± 36.40 Hz. These findings suggest that PMMA-rGO composites hold considerable promise as effective sensing materials for improving QCM sensor performance.

Keywords: QCM sensor, Composites, Reduced graphene oxide, Polymethyl methacrylate, Coffee aroma, Binary solvents, Surface roughness

Introduction

Coffee is one of the popular beverages in the world as well as Indonesia. It has signature aroma that contributes to their taste and flavor [1-5]. In order to assess the quality of coffee or coffee-based products according to their specific aroma, some technologies have been provided, such as colorimetry [6], chromatography-based like LC-MS [7,8] and GC-MS-O [9], and NMR [10-13]. But those advanced technology have several drawback like need sample pre-treatment, expensive, and highly-skilled operator requirements.

Sensor-based technology has been used to detect coffee aroma. Metal oxide semiconductors sensor (MOS) have been used by [14] to differentiate arabica coffee and robusta coffee in the mixture by using support vector machines (SVMs). Other study conducted by [15] developed an electronic nose (e-nose)

tandem with GC-MS and developing the learning model and furthermore extracting the information about coffee aroma the by using machine learning like PCA, ANN, and SVMs. Besides their significant performance, the MOS can be operated only in the high-temperature and not specific.

Electronic nose based on quartz crystal microbalance (QCM) sensors offer advantages such as low cost, high sensitivity and selectivity, and the ability to operate at room temperature [16]. The performance of QCM sensors can be further enhanced using nanomaterials as sensitive layers. Composite is a combination of 2 or more materials with different properties that can be worked synergize. It can be polymer-polymer [17,18], polymer-graphene [19], polymer-metal [20], polymer-graphene-metal [21], etc.

Poly (methyl methacrylate) (PMMA) is a polymer frequently used in sensor technology and biomedical applications, due to its glassy and non-conductive properties [15]. Besides that, PMMA was known because of its chemical stability, ease of film formation, and compatibility with a variety of analytes, particularly volatile organic compounds (VOCs) relevant to environmental and food quality monitoring. PMMA is one of kind glassy polymer, low-cost polymer, lightweight, strong, and non-conductive [22]. PMMA-based QCM sensor have been used for several purposes, such as hydrocarbon detection [23], acetone as biomarker of diabetes mellitus [24], ammonia [25], and humidity [26]. Reduced graphene oxide (rGO) is a 2D carbon-based material with high conductivity, low weight, and rapid electron transfer [22,27]. The combination of PMMA and rGO as a composite material has been used in several applications, such as real-time gamma radiation detection [28], and ammonia detection [25,27].

Several studies have been conducted by using surface-modified QCM sensors to detect food aromas, such as linalool in black tea [29], ocimene aroma in mango by Ghatak *et al.* [30], α-terpinyl acetate in cardamon [31], plants volatile organic compounds [32], and d-limonene from citrus infestation by invasive pest [33]. The combination of PMMA and rGO as a composite material can improve the performance of QCM sensors in detecting specific analytes, such as food aroma. So far, the application of PMMA-rGO coated QCM sensor for coffee aroma detection is rare.

Based on the literature review above, our study aimed to synthesize PMMA and PMMA-rGO composites and their application as sensitive layers on the surface of QCM sensors to detect roasted coffee aromas. The materials were synthesized by using modified in situ polymerization in the presence of a green binary solvent. The robusta coffee was chosen for this experiment, and we used 220℃ as a roasting temperature.

Materials and methods

Materials

All chemicals utilized in this study were high purity and used as received. The amine-functionalized reduced-graphene oxide (rGO-NH_2, 99.9%), azoisobutyronitrile (AIBN), 99.9%), and methyl methacrylate (MMA, 99.9%) were procured from Sigma-Aldrich. Acetone (99%), methanol (99%), and ethanol (99%) were provided by Merck. The synthesis procedure was performed in the presence of demineralized water. The 11 MHz AT-Cut QCM sensor with a dual Ag electrode was acquired from PT Great Microtama, Surabaya.

The synthesis of polymethyl methacrylate (PMMA)

Poly (methyl methacrylate) (PMMA) was synthesized by using one-pot in situ polymerization from Mallik *et al.* [22] and Saeed *et al.* [34] with minor modifications. The 5 mL MMA was mixed with 25 mg AIBN in 1 mL acetone. The green solvent in this synthesis process consisted of ethanol-water, a binary cosolvent system built with a proportion of 1:4 (%v/v). The reaction mixture was maintained at 65 °C under constant stirring for 2 h. The color of the solution changed from colorless to white, indicating the formation of PMMA. Subsequently, the PMMA solid was washed several times with methanol and hot water. Finally, PMMA was dried at 50 °C for 24 h.

The synthesis of composite polymethyl methacrylate-reduced graphene oxide (PMMA-rGO)

The synthesis of the PMMA-rGO composite was carried out using a modified polymerization approach based on established PMMA preparation methods [22]

and [34], with the incorporation of reduced graphene oxide (rGO). Initially, 5 mL of methyl methacrylate (MMA) was combined with 25 mg of azobisisobutyronitrile (AIBN) in 1 mL of acetone to facilitate dissolution. A green cosolvent system consisting of ethanol and water in a 1:4 (% v/v) ratio was used as the reaction medium. The polymerization was conducted at 65°C under continuous stirring for 2 hours, during which the solution gradually changed from colorless to white, indicating the successful formation of PMMA. Once the polymerization had progressed to this stage, 30 mg of rGO was separately dispersed in 1 mL of acetone, subjected to sonication for 10 minutes to ensure proper dispersion, and subsequently introduced into the PMMA solution. The reaction was allowed to proceed for an additional 2 hours to facilitate uniform incorporation of rGO within the polymer matrix. The resulting solid product was repeatedly washed with methanol and hot water to remove any residual impurities. Finally, the PMMA-rGO composite was dried at 50°C for 24 hours to obtain the final material.

Material deposition method

[PMMA and PMMA-rGO coatings were applied to the QCM sensor using a spin-coating process. Firstly, 1 mg of each material was dissolved in 1 mL of acetone to prepare a 1% solution. Then, 50 µL of the solution was dropped onto the sensor surface and spin-coated at 3,000 rpm for 60 seconds. The coating was applied to both sides of the sensor. After deposition, the sensors were heated at 100°C for 60 minutes to improve adhesion.

Characterization

For the surface characteristics, we used an attenuated total reflectance-Fourier transform infrared (ATR-FTIR) instrument to analyze the positions of several functional groups on PMMA and PMMA-rGO. The surface roughness was measured using a non-contact topography measurement system (TMS) of 1,200 µ. Lab from Polytec GmbH, and the morphology of materials was determined using field emission scanning electron microscopy (FESEM) Quanta FEG 650. For the measurement of the initial and post-deposition impedance curve of the QCM sensor, we used an impedance analyzer Bode 100 from Omicron Lab. This measurement was done to check whether the coated QCM sensor still has a good working condition by means that the coating load to the sensor is negligible.

The sensing operation set-up

The QCM sensors coated with PMMA and PMMA-rGO were mounted on a sample holder and placed inside a sealed chamber (Figure 1). A total of 150 grams of Robusta green coffee was loaded into a custom-built lab-scale electronic nose. The roasting process was carried out at 220°C and repeated three times. Sensing measurements were performed over a one-hour period.

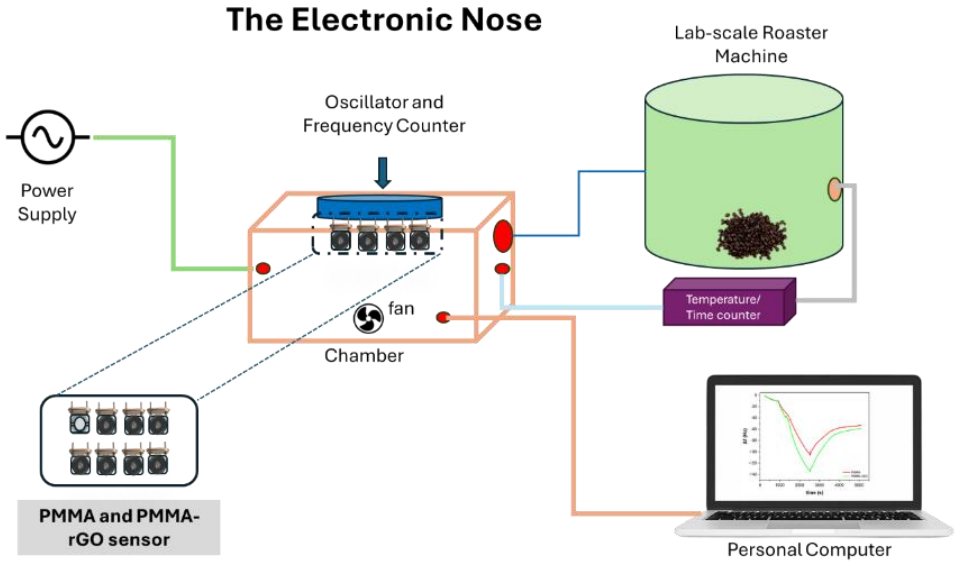

Figure 1 The illustration of electronic nose-based QCM sensors.

Results and discussion

The surface characteristics

ATR-FTIR analysis

The spectra of the MMA, PMMA, rGO, and PMMA-rGO composites are shown in **Figure 2**. There is a slight change in the intensity of the MMA and PMMA peaks around 2.900, 2.800, 1.700, 1.600, 1.400 and 1.200 cm^{-1}. Specifically, the bands around 1.625 cm^{-1} which indicates the alkenyl stretch (-C=C-) in the MMA was not found in the PMMA. This result indicated the conversion of MMA into PMMA. For rGO, the bands around 1.620 and 1.045 cm^{-1} indicate the alkenyl stretch (-C=C-) and (C-O-C) from the epoxides in the rGO structure. Interestingly, the PMMA-rGO spectra showed hydroxyl, carbonyl, ester, and epoxide bands around 3.300, 1.650, 1.460 and 1.020 cm^{-1}, respectively. The bands around 3,300 cm^{-1} indicate the presence of water molecules on PMMA-rGO owing to the synthesis process. The peak-intensity bands of -C-H (stretching) and C=O (stretching) in PMMA-rGO were smaller than those in PMMA. This indicated the presence of rGO in the polymer matrix. This finding is similar to that of previous studies [22,25,27,35].

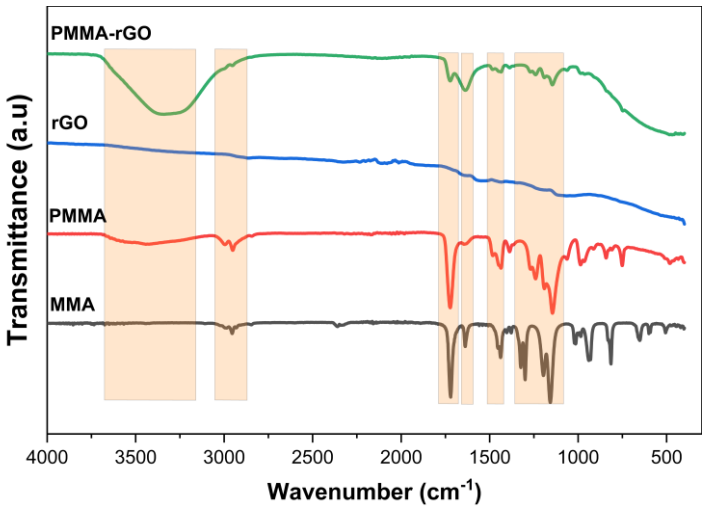

Figure 2 IR spectra for MMA, PMMA, rGO, and PMMA-rGO.

TMS analysis

Table 1 and **Figure 3** show the surface properties of the PMMA-coated- and PMMA-rGO-coated QCM sensors. The QCM sensor with the PMMA coating predominantly consists of a valley pattern because its *Ssk* value is below 0 (*Ssk* < 0), while for the PMMA-rGO, it mostly has a peak pattern (*Ssk* > 0). Based on the surface area roughness (*Sa*), it can be concluded that the PMMA-rGO coated QCM sensor has slightly more roughness than the PMMA-coated QCM. A study by Gaikwad *et al.* [27] revealed that the presence of rGO on the PMMA matrix tremendously increased the surface roughness by a factor of 5, and the surface profiling predominantly consisted of peaks and valleys, which enhanced the response time, recovery time, and response of gases. Hence, the presence of rGO in the PMMA matrix could provide more sites on the surface of the QCM sensor, leading to an increase in the surface roughness. When the surface of QCM sensor was filled with the PMMA only, the mass of PMMA can be contributed to the surface roughness. Contrast, when the PMMA-rGO was deposited on the surface of QCM sensor, the mass of PMMA and rGO are contributed to the surface roughness (**Table 2**). Consequently, the QCM sensor with PMMA-rGO layer could interact with more analytes compared to the PMMA only. The presence of carbonyl groups (C=O) both in PMMA and rGO can be used as sites to interact with the analyte (coffee aroma).

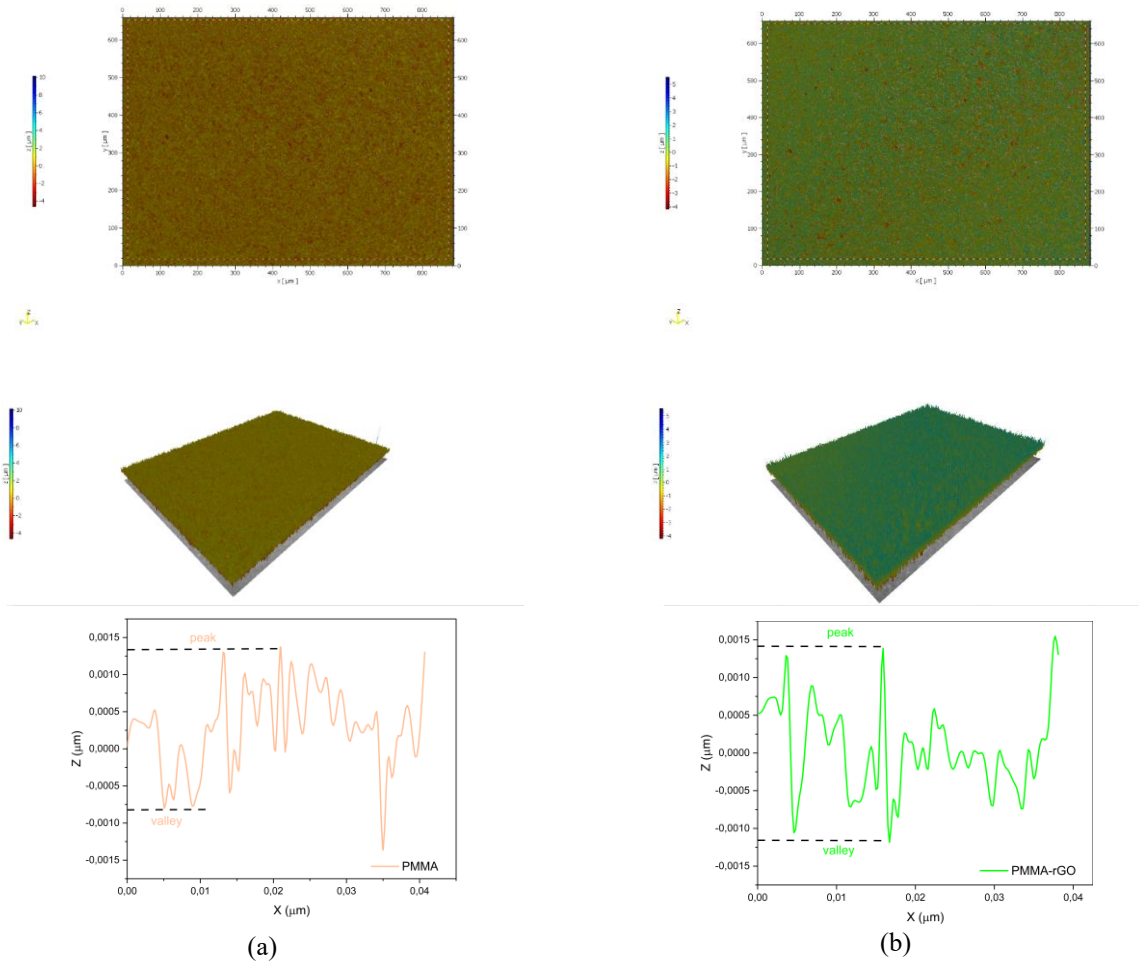

(a) (b)

Figure 3 The Surface Contour of PMMA (a) and PMMA-rGO (b) coated QCM Sensor.

Table 1 The roughness of PMMA-coated and PMMA-rGO-coated QCM.

Coating materials on the QCM surface	Surface roughness parameter		
	Sa (nm)	***Ssk***	***Sz (nm)***
PMMA	446.02 ± 26.19	–0.37 ± 0.39	12,160 ± 3,627.06
PMMA-rGO	493.68 ± 74.23	0.63 ± 1.95	11,193.33 ± 3,731.14

SEM analysis

Based on the SEM data (**Figure 4**), the particle size of PMMA was dominantly around 9 µm with a spherical shape. The layer-by-layer structure is a signature of rGO properties. For PMMA-rGO, the particle size was approximately 3 µm. On PMMA-rGO, it was observed that the PMMA particles were attached to the rGO surface. The presence of rGO as a filler in the PMMA matrix not only improved the properties of the composites but also reduced the particle size of PMMA.

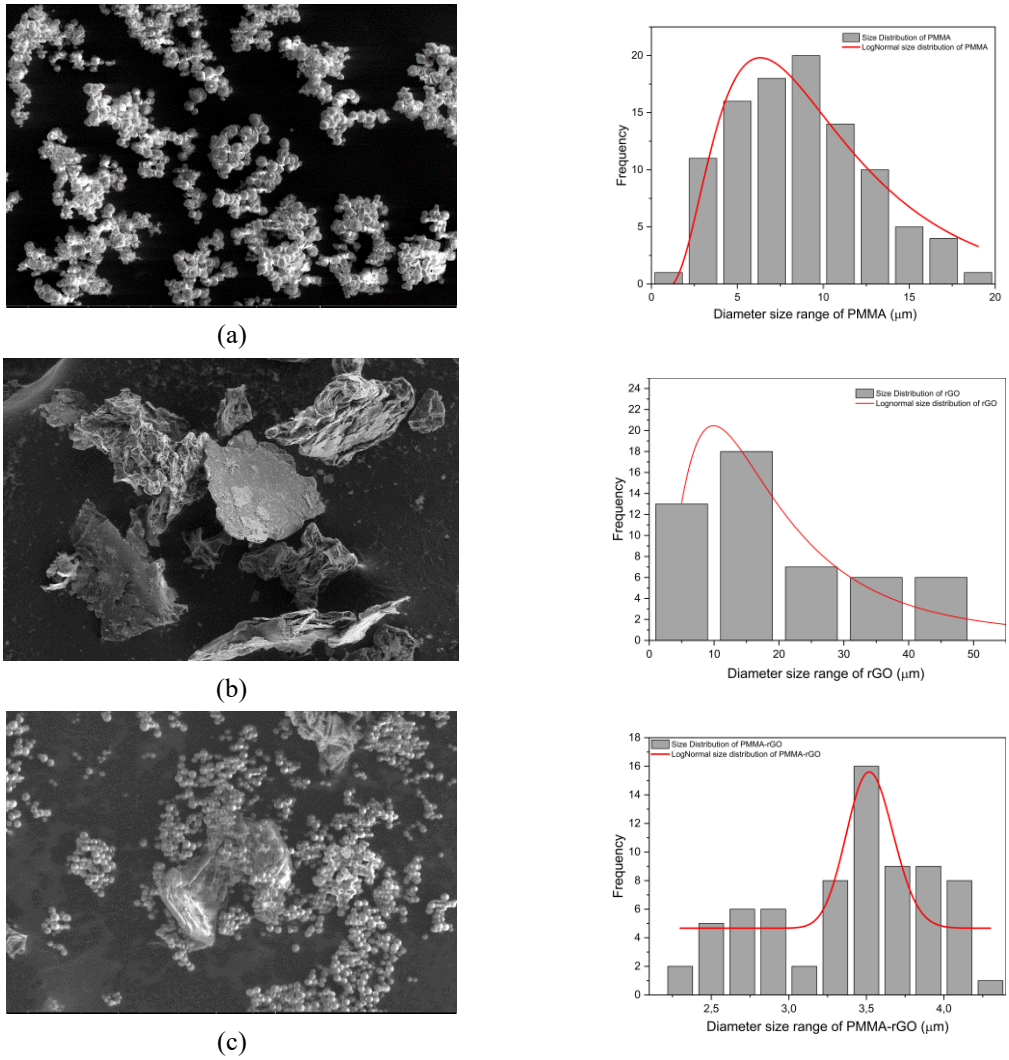

Figure 4 SEM Image for PMMA (a), rGO (b), and PMMA-rGO (c).

The addition of rGO after the PMMA was formed during the synthesis process significantly contributed to the reduced size of the PMMA. rGO may act as a barrier to prevent the PMMA particles from increasing in size. Additionally, the presence of ethanol-water as a cosolvent in the polymerization reaction could result in monodisperse particles with a spherical shape. Hsieh *et al.* [36] in their study revealed that by proper dispersion of monodisperse polystyrene-pyrrole (PS-PPy) microspheres in a water/ethanol cosolvent, result uniform PS-PPy microspheres with significantly reduced size variation, deformation, and aggregation.

The QCM sensor characteristics

Figure 5 and **Table 2** describe the sensor characteristics of PMMA and PMMA-rGO on the surface of the QCM sensor. There was a frequency shift before and after coating. This frequency shift indicates that the thin film successfully covered the surface of the QCM sensor. To determine the amount of PMMA and PMMA-rGO on the surface of the QCM sensor, the Sauerbrey equation [37,38] can be used:

$$\Delta f = -C.\Delta m \quad (1)$$

where Δf is the changing frequency in Hertz, C is the QCM constant, and Δm is amount of coffee aroma (ng) that interacts with the coating materials at the surface of QCM. The amount of PMMA-rGO on the surface of the QCM was higher than that of PMMA.

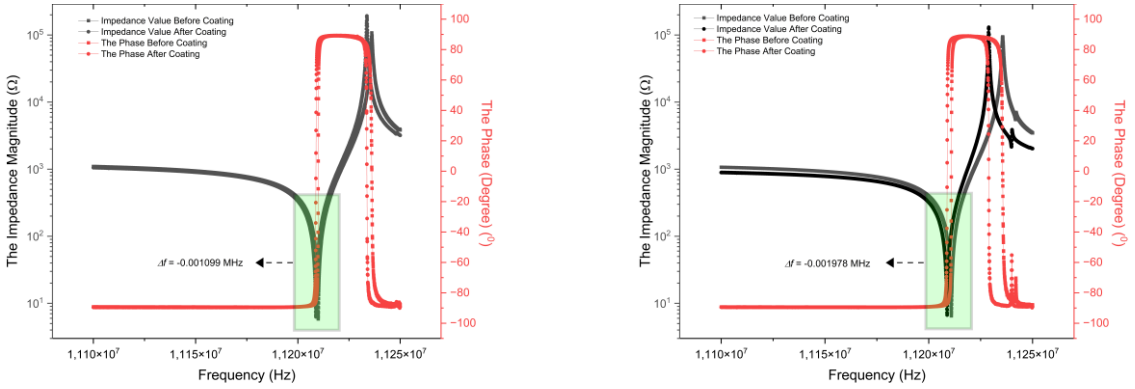

(a) (b)

Figure 5 The Frequency Shift of QCM Sensor Before and After Coating with PMMA (a) and PMMA-rGO (b).

Table 2 The changing frequency and the amount of deposited mass of PMMA and PMMA-rGO on the surface of the QCM sensor.

Sample	Initial frequency, f_0 (Hz)	Frequency after deposition, f_1 (Hz)	The changing frequencies, Δf, (Hz)	The amount of deposited mass, Δm, (ng)
PMMA-coated QCM	11209927	11208828	–1099	0.240
PMMA-rGO-coated QCM	11210842	11208864	–1978	0.432

The sensing performance

The sensing performance of PMMA and PMMA-rGO coated QCM was evaluated at a roasting temperature of 220℃. **Figure 6** shows the different responses of PMMA and PMMA-rGO toward the aroma of roasted coffee. When the coffee aroma was exposed to the chamber, the frequency shift of the PMMA-rGO coated QCM was 74 Hz, while the frequency shift of PMMA was approximately 66 Hz (**Table 3**). The presence of rGO in the polymer matrix significantly increased the sensing performance of the QCM sensors. Reduced graphene oxide may provide more sites for interaction with the analytes (coffee aroma) than PMMA alone. The change in frequency (Δf) for PMMA-rGO was higher than that for PMMA. The decreasing frequency value was linearly related to the amount of coffee aroma (Δm) based on the Sauerbrey equation as shown in Eq. (1) [26,27].

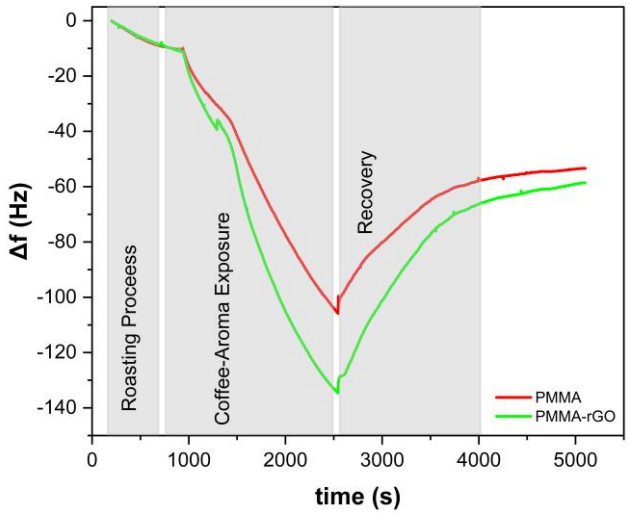

Figure 6 Coffee aroma sensing performance of PMMA- and PMMA-rGO coated QCM sensor at roasting temperature 220 °C.

Table 3 The changing frequency (Δ*f*) and the amount of coffee aroma (Δ*m*) detected by PMMA- and PMMA-rGO coated QCM sensor.

Sample	Roasting Temperature (°C)	Δ*f* (Hz)	Δ*m* (ng)
PMMA-coated QCM	220	–66.05 ± 28.77	6.22 ± 3.05
PMMA-rGO-coated QCM	220	–74.28 ± 36.40	7.13 ± 3.98

The recovery process of PMMA- and PMMA-rGO-coated QCM was poor after exposure to coffee aroma. This clearly suggests a strong interaction between the coating material and aroma at the interface of the QCM sensor. This strong interaction may be affected by the contribution of van der Waals or London forces that formed between PMMA with coffee aroma and PMMA-rGO with coffee aroma. This interaction led to the accumulation of aroma compounds on the surface of the QCM sensor. This accumulation can be detected by the deviation of the frequency before and after the measurement (**Table 4**).

The reproducibility of the QCM sensor with PMMA and PMMA-rGO nanocomposites needs to be improved (**Table 4** and **Figure 7**). The sensitivity of the sensor gradually decreases after several cycles. When the QCM sensors were exposed to coffee aroma, some residues were trapped on the surface of the QCM after measurement. The frequency shift values before and after the measurement in **Table 4** strongly indicate that several coffee aromas may be trapped on the surface of the QCM sensor. This phenomenon can be described as a strong interaction between the coating material and chemical compounds from the coffee aroma. This trapped mass slowly reduced the QCM sensing performance to detect coffee aroma for further experiments.

Table 4 The frequency shift of QCM sensor after several measurements.

Sample	Frequency after deposition, f_1 (Hz)	Frequency after the 1st cycle (Hz)	Frequency after the 3rd cycle (Hz)	Frequency after the 5th cycle (Hz)
PMMA-coated QCM	11208828	11208755	11208388	11207729
PMMA-rGO-coated QCM	11208864	11208791	11208535	11205568

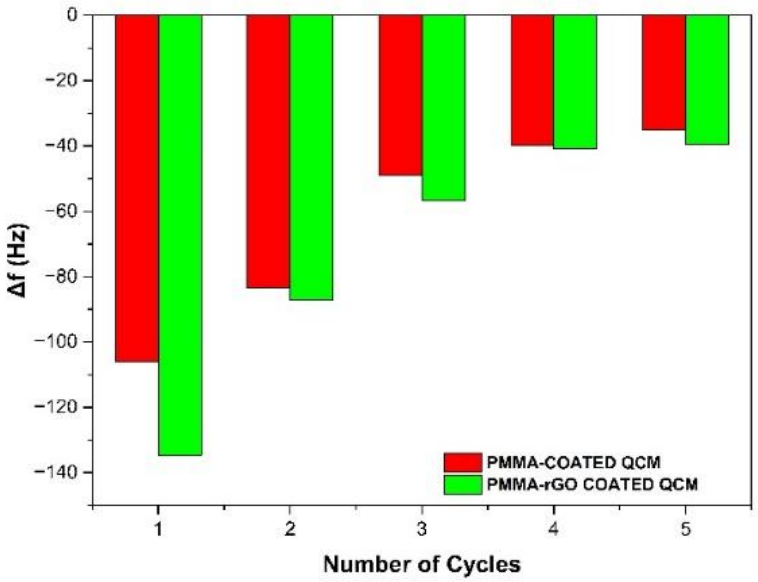

Figure 7 Reproducibility of PMMA-coated (a) and PMMA-rGO-coated (b) QCM sensor.

Conclusions

The PMMA and PMMA-rGO composite were successfully synthesized by using modified *in-situ* polymerization in the presence of green cosolvent system. The PMMA and PMMA-rGO composite-coated QCM sensor can successfully detect roasted coffee aroma, especially at a roasting temperature of 220 °C. The sensing performance of PMMA in the presence of reduced graphene oxide significantly increased the detection of coffee aroma. The PMMA-coated QCM sensor could interact with the coffee aroma denoted by decreasing in frequency (Δf) is –66.05 Hz. While PMMA-rGO coated QCM sensor has a decreasing frequency (Δf) is –74.28 Hz. The presence of rGO in the PMMA matrix provides more sites to interact with coffee aroma compared to PMMA only. However, the sensor performance gradually decreased for both coating materials over many trials. Therefore, the use of this sensor was limited to the next measurement. This issue should be carefully fulfilled before applying it into the real-time application. In addition, the effect of the surface roughness on the sensing ability of the analyte (roasted coffee aroma) still has much work to do, as does their interaction mechanism (between coating materials and coffee aroma).

Acknowledgments

This research is funded by the Professorship Ecosystem Research of Brawijaya University, Indonesia. The authors gratefully acknowledge financial support from the Endowment Fund (LPDP) of The Ministry of Economics, Indonesia.

References

[1] JD Barea-Ramos, G Cascos, M Mesías, J Lozano and D Martín-Vertedor. Evaluation of the olfactory quality of roasted coffee beans using a digital nose. *Sensors* 2022; **22(22)**, 8654.

[2] CH Lee, I Te Chen, HC Yang and YJ Chen. An AI-powered electronic nose system with fingerprint extraction for aroma recognition of coffee beans. *Micromachines (Basel)* 2022; **13(8)**, 1313.

[3] H Purwawangsa, MI Irfany and DA Haq. Indonesian coffee exports' competitiveness and determinants. *Jurnal Manajemen dan Agribisnis* 2024; **21(1)**, 59-71.

[4] F Ashardiono and A Trihartono. Optimizing the potential of Indonesian coffee: A dual market approach. *Cogent Social Sciences* 2024; **10(1)**, 2340206.

[5] M Purnomo, Y Yuliati, A Shinta and FD Riana. Developing coffee culture among indonesia's middle-class: A case study in a coffee-producing country. *Cogent Social Sciences* 2021; **7(1)**, 1949808.

[6] BA Suslick, L Feng and KS Suslick. Discrimination of complex mixtures by a colorimetric sensor array: coffee aromas. *Anal Chem* 2010; **82(5)**, 2067-2073.

[7] S Sittipod, E Schwartz, L Paravisini and DG Peterson. Identification of flavor modulating compounds that positively impact coffee quality. *Food Chemistry* 2019; **301**, 125250.

[8] L Xu, F Lao, Z Xu, X Wang, F Chen, X Liao, A Chen and S Yang. Use of liquid chromatography quadrupole time-of-flight mass spectrometry and metabolomic approach to discriminate coffee brewed by different methods. *Food Chemistry* 2019; **286**, 106-112.

[9] R Crnjar, P Solari and G Sollai**.** The human nose as a chemical sensor in the perception of coffee aroma: individual variability. *Chemosensors* 2023; **11(4)**, 0248.

[10] F Wei, K Furihata, T Miyakawa and M Tanokura. A pilot study of NMR-based sensory prediction of roasted coffee bean extracts. *Food Chem* 2014; **152**, 363-369.

[11] M Defernez, E Wren, A D Watson, Y Gunning, I J Colquhoun, G Le Gall, D Williamson and E K Kemsley. Low-field ^{1}H NMR spectroscopy for distinguishing between arabica and robusta ground roast coffees. *Food Chemistry* 2017; **216**, 106-113.

[12] R Consonni, D Polla and L R Cagliani. Organic and conventional coffee differentiation by NMR spectroscopy. *Food Control* 2018; **94**, 284-288.

[13] JCC Freitas, M Ejaz, AT Toci, W Romão and YZ Khimyak. Solid-state NMR spectroscopy of roasted and ground coffee samples: Evidences for phase heterogeneity and prospects of applications

in food screening. *Food Chemistry* 2023; **409**, 135317.

[14] K Brudzewski, S Osowski and A Dwulit. Recognition of coffee using differential electronic nose. *IEEE Transactions on Instrumentation and Measurement* 2012; **61(6)**, 1803-10.

[15] CG Viejo, E Tongson and S Fuentes. Integrating a low-cost electronic nose and machine learning modelling to assess coffee aroma profile and intensity. *Sensors* 2021; **21**, 1-15.

[16] Q Zhou, C Zheng, L Zhu and J Wang. A review on rapid detection of modified quartz crystal microbalance sensors for food: Contamination, flavour and adulteration. *TrAC Trends in Analytical Chemistry* 2022; **157**, 116805.

[17] L Katriani, R Aflaha, AH As'ari, P Nurwantoro, R Roto and K Triyana. Nanofiber-coated quartz crystal microbalance with chitosan overlay for highly sensitive room temperature ammonia gas sensor. *Microchemical Journal* 2024; **206**, 111532.

[18] K Triyana, A Sembiring, A Rianjanu, SN Hidayat, R Riowirawan, T Julian, A Kusumaatmaja, I Santoso and R Roto. Chitosan-based quartz crystal microbalance for alcohol sensing. *Electronics* 2018; **7(9)**, 181.

[19] A Trajcheva, N Politakos, BT Pérez, Y Joseph, JB Gilev and R Tomovska. QCM nanocomposite gas sensors - Expanding the application of waterborne polymer composites based on graphene nanoribbon. *Polymer* 2021; **213**, 123335.

[20] Y Hu, H Xing, G Li and M Wu. Magnetic imprinted polymer-based quartz crystal microbalance sensor for sensitive label-free detection of methylene blue in groundwater. *Sensors* 2020; **20(9)**, 5506.

[21] D Zhang, D Wang, X Zong, G Dong and Y Zhang. High-performance QCM humidity sensor based on graphene oxide/tin oxide/polyaniline ternary nanocomposite prepared by in-situ oxidative polymerization method. *Sensors and Actuators B: Chemical* 2018; **262**, 531-41.

[22] AK Mallik AK, ML Habib, FN Robel, M Shahruzzaman, P Haque, MM Rahman, V Devanath, DJ Martin, AK Nanjundan, Y Yamauchi, M Takafuji and H Ihara. Reduced graphene oxide (rGO) prepared by metal-induced reduction of graphite oxide: Improved conductive behavior of a poly(methyl methacrylate) (PMMA)/rGO composite. *ChemistrySelect* 2019; **4(27)**, 7954-7958.

[23] C White, B Pejcic, M Myers and X Qi. Development of a plasticizer-poly(methyl methacrylate) membrane for sensing petroleum hydrocarbons in water. *Sensors and Actuators B: Chemical* 2014; **193**, 70-77.

[24] M Rodríguez-Torres, V Altuzar, C Mendoza-Barrera, G Beltrán-Pérez, J Castillo-Mixcóatl and S Muñoz-Aguirre. Acetone detection and classification as biomarker of diabetes mellitus using a quartz crystal microbalance gas sensor array. *Sensors* 2023; **23(24)**, 9823.

[25] A Raza, R Abid, I Murtaza and T Fan. Room temperature NH3 gas sensor based on PMMA/RGO/ZnO nanocomposite films fabricated by in-situ solution polymerization. *Ceramics International* 2023; **49(16)**, 27050-27059.

[26] NA Tehrani, IC Esfahani and H Sun. Simultaneous humidity and temperature measurement with micropillar enhanced QCM sensors. *Sensors and Actuators A: Physical* 2024; **366**, 115039.

[27] SS Gaikwad, AS Khune, NN Ingle NN and MD Shirsat. Chemiresistive sensor based on PMMA/rGO composite for detection ammonia. *Sensors and Actuators A: Physical* 2024; **377**, 115665.

[28] S Feizi, A Mehdizadeh, MA Hosseini, SA Jafari and P Ashtari. Reduced graphene oxide/polymethyl methacrylate (rGO/PMMA) nanocomposite for real time gamma radiation detection. *Nuclear Instruments and Methods in Physics Research Section A: Accelerators, Spectrometers, Detectors and Associated Equipment* 2019; **940**, 72-77.

[29] P Sharma, A Ghosh, B Tudu, LP Bhuyan, P Tamuly, N Bhattacharyya, R Bandyopadhyay and A Chatterjee. Detection of linalool in black tea using a quartz crystal microbalance sensor. *Sensors and Actuators B: Chemical* 2014; **190**, 318-325.

[30] B Ghatak, SB Ali, B Tudu, P Pramanik, S Mukherji and R Bandyopadhyay. Detecting ocimene in mango using mustard oil based quartz

crystal microbalance sensor. *Sensors and Actuators B: Chemical* 2019; **284**, 514-524.

[31] N Debabhuti, S Neogi, S Mukherjee, A Dhar, P Sharma, RL Vekariya, MP Sarkar, B Tudu B, N Bhattacharyya, R Bandyopadhyay and M Muddassir. Development of QCM sensor to detect α-terpinyl acetate in cardamom. *Sensors and Actuators A-physical* 2021; **319**, 112521.

[32] Z Wang, W Chen, S Gu, J Wang and Y Wang. Discrimination of wood borers infested Platycladus orientalis trunks using quartz crystal microbalance gas sensor array. *Sensors and Actuators B: Chemical* 2020; **309**, 127767.

[33] T Wen, M Sang, M Wang, L Han, Z Gong, X Tang, X Long, H Xiong and H Peng. Rapid detection of d-limonene emanating from citrus infestation by Bactrocera dorsalis (Hendel) using a developed gas-sensing system based on QCM sensors coated with ethyl cellulose. *Sensors and Actuators B: Chemical* 2021; **328**, 129048.

[34] PA Saeed PA and A Sujith. A simple approach to develop conductive poly(methyl methacrylate)-reduced graphene oxide composite with segregated network. *Polymer Bulletin* 2024; **81**, 8917-8931.

[35] D Tumnantong, S Poompradub and P Prasassarakich. Conductive NR/PMMA-RAFT-CNT-rGO composites and their morphological, mechanical, and electrical properties. *Journal of Industrial and Engineering Chemistry* 2024; **141(12)**, 501-511.

[36] TL Hsieh, PS Hung, CJ Wang, YS Chou and PW Wu. Controlled synthesis of uniform hollow polypyrrole microcapsules by a cosolvent approach. *SN Applied Sciences* 2019; **1(4)**, 319.

[37] X Qiao, X Zhang, Y Tian and Y Meng. Progresses on the theory and application of quartz crystal microbalance. *Applied Physics Reviews* 2016; **3**, 031106.

[38] G Sauerbrey. Verwendung von Schwingquarzen zur Wägung dünner Schichten und zur Mikrowägung. *Zeitschrift für Physik* 1959; **155**, 206-222.